



ChemComm

**Antiaromaticity Gain Increases Potential for n-Type Charge Transport in Hydrogen-Bonded  $\pi$ -Conjugated Cores**

|               |                          |
|---------------|--------------------------|
| Journal:      | <i>ChemComm</i>          |
| Manuscript ID | CC-COM-12-2019-009670.R1 |
| Article Type: | Communication            |
|               |                          |

SCHOLARONE™  
Manuscripts

## Antiaromaticity Gain Increases Potential for *n*-Type Charge Transport in Hydrogen-Bonded $\pi$ -Conjugated Cores

Z. Wen, J. I. Wu\*

 Received 00th January 20xx,  
 Accepted 00th January 20xx

DOI: 10.1039/x0xx00000x

**Abstract.** Density functional theory computations suggest that formally non-aromatic organic dyes, like diketopyrrolopyrrole, naphthodipyrrolidone, indigo, and isoindigo, show increased  $[4n]$   $\pi$ -antiaromatic character and decreased LUMO orbital energies upon hydrogen bonding, making them suitable molecular candidates for applications in *n*-type organic field effect transistors.

Antiaromatic compounds are gaining traction as promising candidates for the design of *n*-type organic field effect transistors (OFET), because of their potential to have low LUMO energy levels, narrow HOMO-LUMO gaps, and high conductivity.<sup>1–4</sup> But formally antiaromatic—cyclic  $[4n]$   $\pi$ -conjugated—cores can sometimes be too reactive (e.g., pentalene cores easily dimerize) to be useful unless stabilized by fused benzenoid rings. Some successful examples of  $[4n]$   $\pi$ -conjugated *n*-type OFET candidates include expanded pentalenes, indacenes, and indenofluorenes.<sup>5–8</sup> In this paper, we consider a class of non-aromatic organic dyes, including: diketopyrrolopyrrole (DPP), naphthodipyrrolidone (NDP), indigo, and isoindigo, (Figure 1), which show *n*-type behavior.<sup>9,10,11</sup> We show that when these compounds self-assemble through hydrogen bonding interactions, they show increased antiaromaticity and lower LUMO energy levels.

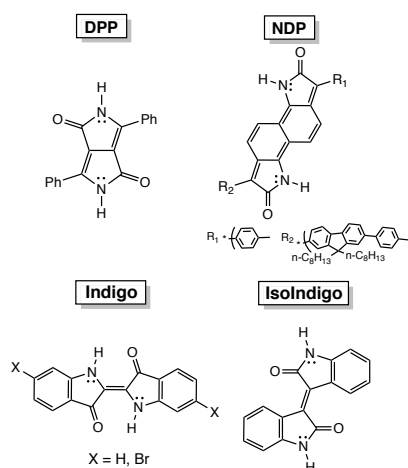


**Figure 1.** Formally non-aromatic  $\pi$ -conjugated cores.

University of Houston, Department of Chemistry.

\* footnotes.

Electronic Supplementary Information (ESI) available: [details of any supplementary information available should be included here]. See DOI: 10.1039/x0xx00000x

Organic dyes like DPP, NDP, indigo, and isoindigo, are traditionally thought to be poor candidates for applications as organic electronics, as the N–H and C=O groups were considered to disrupt  $\pi$ -conjugation thereby lowering electron or hole mobility. But recent works from Głowacki and others have shown that N–H and C=O containing pigments like acridones and indigos can exhibit high charge mobilities, rivaling those of traditional acene-based OFETs.<sup>12–15</sup> Zhu and co-workers reported that hydrogen bonding increases the hole mobilities of indigo ( $4.06 \times 10^{-6}$  to  $3.24 \times 10^{-5}$  cm<sup>2</sup>/Vs), isoindigo ( $1.91 \times 10^{-5}$  to  $9.05 \times 10^{-5}$  cm<sup>2</sup>/Vs),<sup>9</sup> and DPP ( $1.30 \times 10^{-4}$  to  $7.89 \times 10^{-4}$  cm<sup>2</sup>/Vs), compared to their t-boc protect analogs preclude of hydrogen bonding sites.<sup>10</sup> NDP displayed significant increase in electron mobility (from  $2.40 \times 10^{-4}$  to 0.01 cm<sup>2</sup>/Vs) upon t-boc removal.<sup>11</sup>

Here we show that the high charge mobility of these organic dyes arise from increased antiaromatic character in the  $\pi$ -conjugated cores upon forming hydrogen bonding interactions. DPP, NDP, indigo, and isoindigo, are formally non-aromatic. But hydrogen bonding interactions at the N–H and C=O sites can polarize the ring  $\pi$ -electrons to increase  $[4n]$   $\pi$ -antiaromatic character. Consider the two isomers of diketopyrrole shown in Figure 2. Both rings have four ring  $\pi$ -electrons and two exocyclic carbonyl groups that breach cyclic  $\pi$ -electron delocalization. Upon hydrogen bonding, the ring  $\pi$ -electrons are polarized, resulting in increased resonance contribution from a formally  $[4n]$  cyclic delocalized structure (see Figure 2).

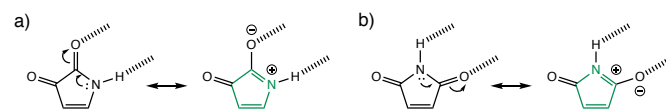


**Figure 2.** Hydrogen bonding interactions increase antiaromaticity (i.e.,  $[4n]$   $\pi$ -electron delocalization) in diketopyrroles.

Hydrogen bonded DPP, NDP, indigo, and isoindigo, exhibit similar antiaromaticity gain. DPP has ten ring  $\pi$ -electrons in the monomeric form (if one considers the  $\pi$ -electrons on the carbon atoms of the C=O groups). When hydrogen bonded, the  $\pi$ -electrons of the C=O groups are polarized towards the oxygen atom, giving rise to pseudo eight ring  $\pi$ -electrons. NDP has 18 ring  $\pi$ -electrons in the monomeric form and can be considered to have 16 ring  $\pi$ -electrons when the C=O groups are polarized by hydrogen bonds. In indigo and isoindigo the central CC bond connects a pair of ten ring  $\pi$ -electron moieties, that can be viewed as eight ring  $\pi$ -electron cycles when the C=O groups are hydrogen bonded.

Three computational models were considered: 1) the monomer of the  $\pi$ -conjugated core, 2) the central unit of a hydrogen bonded trimer of the  $\pi$ -conjugated core, and 3) a  $[4n]$   $\pi$ -electron tautomer of the  $\pi$ -conjugated core (approximating the upper bound electronic effect of a highly polarized monomer). Computed nucleus independent chemical shifts (NICS) quantified the aromaticity and antiaromaticity of the individual rings, and time-dependent density functional theory (TD-DFT) computations were performed to estimate the HOMO and LUMO levels of each model system.<sup>16-18</sup> As shown in Figure 3, hydrogen bonding interactions lower the LUMO levels of all  $\pi$ -conjugated cores, and the  $[4n]$  antiaromatic tautomers display even lower LUMO levels. Details of the HOMO and LUMO levels are included in the Supporting Information (SI).

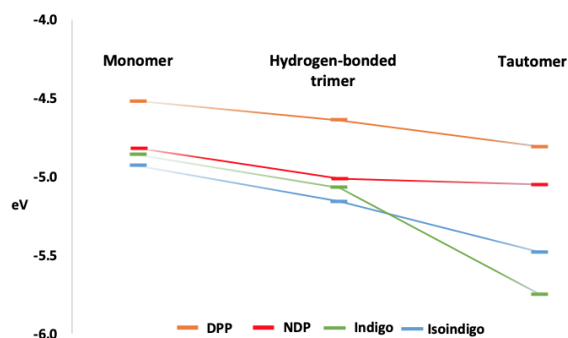


**Figure 3.** Computed LUMO energy levels for the monomers, central units of hydrogen bonded trimers, and  $[4n]$  tautomers of DPP (orange), NDP (red), indigo (green), and isoindigo (blue).

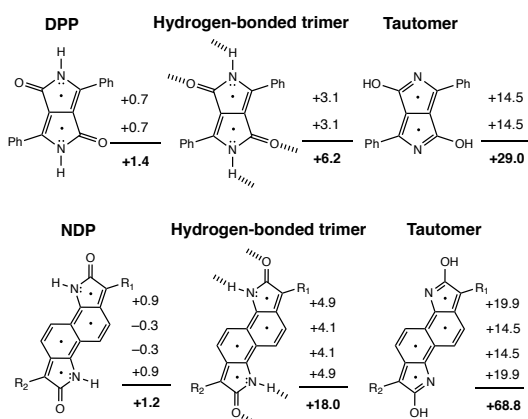


**Figure 4.** Computed NICS(1)<sub>zz</sub> values and sum of NICS(1)<sub>zz</sub> values (in ppm) for the five and six membered rings of DPP and NDP, in the monomer, hydrogen-bonded, and tautomeric forms.

According to computed nucleus independent chemical shifts (NICS), all of the non-aromatic  $\pi$ -conjugated cores become more antiaromatic upon hydrogen bonding, and even more so upon tautomerizing to the  $[4n]$  isomer. NICS(1)<sub>zz</sub> values were computed at 1 Å above each of the ring centers and include only shielding tensor components from the out-of-plane “zz” direction. Negative NICS(1)<sub>zz</sub> values indicate aromaticity, positive NICS(1)<sub>zz</sub> values indicate antiaromaticity. NICS(1)<sub>zz</sub> values close to zero suggest a non-aromatic ring. Based on computed NICS(1)<sub>zz</sub>, the five and six membered ring moieties of DPP and NDP are non-aromatic in the monomer form (NICS(1)<sub>zz</sub> values between -1 and +1 ppm), and become weakly

antiaromatic upon hydrogen bonding (+3 to +5 ppm). NICS(1)<sub>zz</sub> values for the five and six membered ring moieties in the  $[4n]$   $\pi$ -tautomers are even more positive (+15 to +20 ppm) (see Figure 4).

Indigo and isoindigo also show increased antiaromatic character upon hydrogen bonding and tautomerization to the  $[4n]$  isomers (Figure 5). For both systems, the six membered rings are six  $\pi$ -electron aromatic (i.e., two Clar sextets each), and the five membered rings are weak to non-aromatic. Hydrogen bonding reduces the aromatic character of the six membered rings, and increases the antiaromatic character of the five membered rings (NICS(1)<sub>zz</sub> values between +3 and +7 ppm). The  $[4n]$  tautomers of indigo and isoindigo lose even more aromatic character, as the five membered rings become more antiaromatic (NICS(1)<sub>zz</sub> values between +12 and +19 ppm).

Note the significant gain in antiaromaticity in the  $[4n]$  tautomer of indigo. As shown in Figure 5, both indigo and isoindigo have two Clar sextets (i.e., a cyclic delocalization of six  $\pi$ -electrons that resist disruption). But the  $[4n]$  tautomer of indigo loses both Clar sextets (see Lewis structure in Figure 5), while the  $[4n]$  tautomer of isoindigo retains both. This difference also is reflected in the especially low LUMO energy for  $[4n]$  indigo (-5.75 eV, Figure 3). Previous works have shown that Clar sextet patterns can influence the HOMO and LUMO energy levels of  $\pi$ -conjugated compounds; lower numbers of Clar sextet are often associated with smaller HOMO-LUMO gaps and lower LUMO energy levels.<sup>19-21</sup>

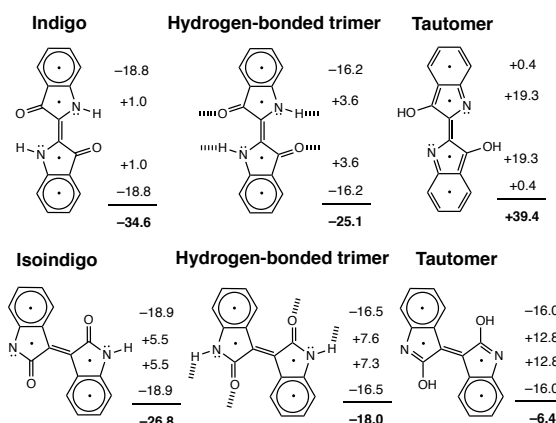


**Figure 5.** Computed NICS(1)<sub>zz</sub> values and sum of NICS(1)<sub>zz</sub> values (in ppm) for the five and six membered rings of indigo and isoindigo, in the monomer, hydrogen-bonded, and tautomeric forms (note Clar sextets).

Gauge-including magnetically induced current (GIMIC)<sup>22</sup> plots of indigo and isoindigo were computed to visualize the effects of arrangements of benzofusion on the numbers of possible Clar sextets in the  $[4n]$  tautomers. Indigo displays strong diatropic (clockwise) ring currents around the six membered rings (i.e., two Clar sextets) and weak paratropic (anti-clockwise) ring currents around the five membered rings (Figure 6a). In the  $[4n]$  tautomer, the diatropic ring currents weaken significantly (in line with a disappearing Clar sextet) and the paratropic currents at the five membered rings become stronger (Figure 6b). GIMIC plots for isoindigo and its  $[4n]$  tautomer look more similar. Both show notable diatropic (clockwise) ring currents around the six membered rings (i.e., two Clar sextets) and weak paratropic (anti-clockwise) ring currents around the five membered rings (Figure 7).

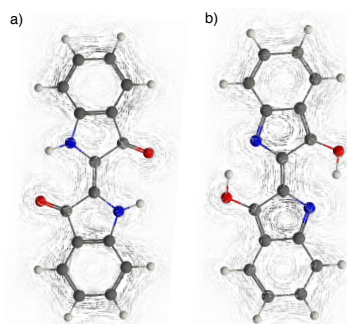


**Figure 6.** GIMIC plots for a) indigo and its b)  $[4n]$  tautomer.

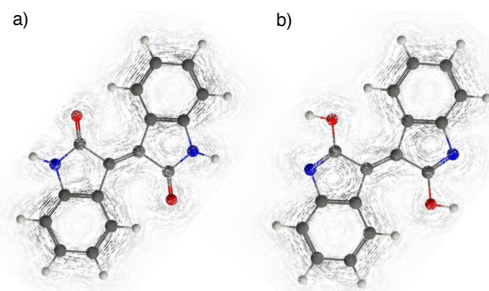


**Figure 7.** GIMIC plots for a) isoindigo and its b)  $[4n]$  tautomer.

Substituents effect also can influence the antiaromaticity and potential  $n$ -type behavior of  $[4n]$   $\pi$ -conjugated cores. For example, tyrian purple (6,6'-dibromoindigo, see Figure 1) is known to exhibit a 40 times higher electron mobility than that of unsubstituted-indigo in OFET devices.<sup>14,23</sup> Our calculations suggest that the lower LUMO level of tyrian purple ( $-5.17$  eV) vs. indigo ( $-4.86$  eV), may be explained by reduced aromaticity (sum of NICS( $1_{zz}$ ) =  $-31.9$  ppm, compared to  $-34.6$  ppm for indigo). Orbital energies and NICS( $1_{zz}$ ) results for tyrian purple are included in SI.

| Model A     | Hydrogen-bonded trimer | Tautomer    |
|-------------|------------------------|-------------|
|             |                        |             |
| +11.0       | +14.7                  | +72.3       |
| -16.6       | -12.4                  | +39.7       |
| -23.7       | -20.9                  | +14.0       |
| <hr/> -29.3 | <hr/> -18.6            | <hr/> +126  |
| Model B     | Hydrogen-bonded trimer | Tautomer    |
|             |                        |             |
| +5.8        | +7.7                   | +8.8        |
| -24.5       | -23.1                  | -22.0       |
| -27.7       | -27.3                  | -27.2       |
| <hr/> -46.4 | <hr/> -42.7            | <hr/> -40.4 |

**Figure 8.** Computed NICS( $1_{zz}$ ) values and sum of NICS( $1_{zz}$ ) values (in ppm) for two  $\pi$ -conjugated core, model A and model B, in the monomer, hydrogen-bonded, and tautomeric forms.

Two compounds, shown as models A and B in Figure 8, also illustrate the effect of how Clar sextets influence the antiaromaticity and LUMO energy levels of the hydrogen bonded monomers. Antiaromaticity gain is more prominent when the hydrogen bonded

compound loses a Clar sextet (see model A, cf. computed NICS( $1_{zz}$ ) for model B). Accordingly, changes in the energy of the LUMO for model A (LUMO:  $-4.86$  eV vs.  $-6.22$  eV in the tautomer) is more pronounced compared to that of model B (LUMO:  $-4.39$  eV vs.  $-4.44$  eV in the tautomer).

Hydrogen bonding interactions can be used to introduce  $[4n]$  antiaromatic character into formally non-aromatic  $\pi$ -conjugated cores, to improve orbital energy levels for  $n$ -type charge transport behavior. Of course, changes in the HOMO-LUMO gaps and LUMO energy levels are just primitive indicators of improved OFET behavior. Future works will take into account the effect of hydrogen bonding on band structure and conductivity in more sophisticated models. Nevertheless, we show that the relationship—between hydrogen bonding and antiaromaticity—is relevant to the molecular design of  $n$ -type OFET compounds and may be used to expand the library of potential candidates to non-aromatic cores with “near  $[4n]$   $\pi$ -conjugated” topologies.

We thank the National Science Foundation (NSF) (CHE-1751370) and the National Institute of General Medical Sciences (NIGMS) of the National Institute of Health (R35GM133548) for grant support. Support for this work also was provided by resources of the uHPC managed by the University of Houston and acquired through grant support from the NSF (CHE-1531814).

## Method

Geometries of all monomers, hydrogen-bonded trimers, and tautomers were optimized with  $C_s$  constraint, except for the hydrogen-bonded trimer of isoindigo (optimized with  $C_1$  symmetry). All geometries were optimized in the gas-phase at the B3LYP<sup>24</sup>/6-311+G(d,p) level, employing Gaussian16.<sup>25</sup> HOMO and LUMO energies were calculated at TD- $\omega$ B97X-D<sup>26</sup>/6-311+G(d,p). HOMO-LUMO gaps were derived from HOMO to LUMO excitation energies. NICS( $1_{zz}$ ) values were computed at PW91PW91/IGLOIII. Magnetically induced current density plots were computed using the GIMIC method.

## Notes and references

1. R. Breslow, *Acc. Chem. Res.*, 1973, **6**, 393–398.
2. T. M. Krygowski, M.K.Cyrański, Z. Czarnocki, G.Häfelinger and A. R. Katritzky, *Tetrahedron*, 2000, **56**, 1783–1796.
3. K. B. Wiberg, *Chem. Rev.*, 2001, **101**, 1317–1332.
4. S. Fujii, S. Marqués-González, J.-Y. Shin, H. Shinokubo, T. Masuda, T. Nishino, N. P. Arasu, H. Vázquez and M. Kiguchi, *Nat. Commun.*, 2017, **8**, 15984.
5. M. Nakano, I. Osaka and K. Takimiya, *J. Mater. Chem. C*, 2015, **3**, 283–290.
6. G. Dai, J. Chang, L. Jing and C. Chi, *J. Mater. Chem. C*, 2016, **4**, 8758–8764.
7. D. T. Chase, A. G. Fix, S. J. Kang, B. D. Rose, C. D. Weber, Y. Zhong, L. N. Zakharov, M. C. Lonergan, C. Nuckolls and M. M. Haley, *J. Am. Chem. Soc.*, 2012, **134**, 10349–10352
8. J. L. Marshall, K. Uchida, C. K. Frederickson, C. Schutt, A. M. Zeidell, K. P. Goetz, T. W. Finn, K. Jarolimek, L. N. Zakharov, C. Risko, R. Herges, O. D. Jurchescu and M. M. Haley, *Chem. Sci.*, 2016, **7**, 5547–5558
9. C. Liu, S. Dong, P. Cai, P. Liu, S. Liu, J. Chen, F. Liu, L. Ying, T. P. Russell, F. Huang and Y. Cao, *ACS Appl. Mater. Interfaces*, 2015, **7**, 9038–9051.

10. E. D. Głowacki, H. Coskun, M. A. Blood-Forsythe, U. Monkowius, L. Leonat, M. Grzybowski, D. Gryko, M. S. White, A. Aspuru-Guzik and N. S. Sariciftci, *Org. Electron.*, 2014, **15**, 3521–3528.
11. H. Zhang, K. Yang, Y.-M. Chen, R. Bhatta, M. Tsige, S. Z. D. Cheng and Y. Zhu, *Macromol. Chem. Phys.*, 2017, **218**, 1600617.
12. E. D. Głowacki, L. Leonat, M. Irimia-Vladu, R. Schwödiauer, M. Ullah, H. Sitter, S. Bauer and N. S. Sariciftci, *Appl. Phys. Lett.*, 2012, **101**, 023305.
13. E. D. Głowacki, G. Romanazzi, C. Yumusak, H. Coskun, U. Monkowius, G. Voss, M. Burian, R. T. Lechner, N. Demitri, G. J. Redhammer, N. Sünger, G. P. Suranna and S. Sariciftci, *Adv. Funct. Mater.*, 2015, **25**, 776–787.
14. E. D. Głowacki, G. Voss and N. S. Sariciftci, *Adv. Mater.*, 2013, **25**, 6783–6800.
15. E. D. Głowacki, M. Irimia-Vladu, M. Kaltenbrunner, J. Gsiorowski, M. S. White, U. Monkowius, G. Romanazzi, G. P. Suranna, P. Mastrorilli, T. Sekitani, S. Bauer, T. Someya, L. Torsi and N. S. Sariciftci, *Adv. Mater.*, 2013, **25**, 1563–1569.
16. P. v. R. Schleyer, C. Maerker, A. Dransfeld, H. Jiao and N. J. R. v. E. Hommes, *J. Am. Chem. Soc.*, 1996, **118**, 6317–6318.
17. Z. Chen, C. S. Wannere, C. Corminboeuf, R. Puchta and P. v. R. Schleyer, *Chem. Rev.*, 2005, **105**, 3842–3888.
18. J.-L. Bredas, *Mater. Horiz.*, 2014, **1**, 17–19.
19. K. J. Thorley and J. E. Anthony, *Isr. J. Chem.*, 2014, **54**, 642–649.
20. C. Aumaitre and J. F. Morin, *Chem. Rec.*, 2019, **19**, 1142–1154.
21. Y. Ruiz-Morales, *J. Phys. Chem. A*, 2004, **108**, 10873–10896.
22. M. Rauhalahhti, S. Taubert, D. Sundholm, V. Liegeois, *Phys. Chem. Chem. Phys.*, 2017, **19**, 7124–7131.
23. E. D. Głowacki, G. Voss, L. Leonat, M. I. Vladu, S. Bauer and N. S. Sariciftci, *Isr. J. Chem.*, 2012, **52**, 540–551.
24. S. Grimme, J. Antony, S. Ehrlich and H. Krieg, *J. Chem. Phys.*, 2010, **132**, 154104.
25. Gaussian 16, Revision A. 03, Gaussian, Inc., Wallingford CT, 2016.
26. J.-D. Chai and M. Head-Gordon, *Phys. Chem. Chem. Phys.*, 2008, **10**, 6615–6620.